Ballistic versus electronic processes in ion-induced nanostructuring of ionic surfaces

F. Krok,* S. R. Saeed,† Z. Postawa, and M. Szymonski
Research Center for Nanometer-Scale Science and Advanced Materials (NANOSAM), Faculty of Physics, Astronomy and Applied Computer Science, Jagiellonian University, ul. Reymonta 4, 30-059 Krakow, Poland
(Received 31 March 2009; published 25 June 2009)

High-resolution noncontact atomic force microscopy in UHV has been used for characterization of KBr(001) surface morphology development due to an oblique incidence of low-energy ion beams (4 keV He^+ and Ar^+ at 75°). We have found several features of the process directly related to the ionic nature of halide surfaces, such as formation of two-dimensional (2D) pits and rectangular 2D epitaxial adislands on the initially atomically flat terraces. At low bombardment fluence the evolution of the 2D pits proceeds along main surface crystallographic directions. Such behavior is typical for the electron stimulated desorption (ESD) process, well-known from electron and photon irradiation experiments. No epitaxial adislands formation by ESD or by ion impact has been reported so far. For prolonged ion bombardment surface topography transforms into a regular network of grooves and rims (a ripple structure) oriented parallel to the incident beam. Such a structure has been observed for many other materials (metals and semiconductors), with a major distinction, however, that for KBr the ripples are composed of small nanosize crystallites with a persistent long-range order of the (001) surface. We have demonstrated that the fluence threshold for a transition from a random network of 2D pits and adislands into a well-oriented crystalline nanoripple structure is directly related to the balance between the electronic and ballistic stopping of the impinging ions. The theoretical interpretation of our observations is based on an atomistic approach to the ion-solid interaction and supplementary molecular-dynamics computer simulations of a single-ion impact on flat and atomic step covered surfaces. In particular, the computer simulations demonstrate that the sputtering yield for ions impinging against the ascending step edges on the irradiated surface are much greater than the ones obtained for the descending step bombardment.

DOI: 10.1103/PhysRevB.79.235432 PACS number(s): 68.35.B−

I. INTRODUCTION

The formation of ripple structures developing on surfaces irradiated with low-energy ion beam has drawn considerable attention during last few years.[1] It has been found that the dynamics of the ripple formation strongly depends on the kinetic energy and the impact angle of the projectile. It has also been shown that the presence of this process is not material related. So far, the formation of ripples has been observed on metal,[2,3] semiconductor,[4–8] and insulator surfaces.[9] The first attempt to explain the mechanism of ripple formation was a model proposed by Bradley and Harper (BH).[10] The model was based on a Sigmund's linear cascade approximation of sputtering in amorphous targets.[11] According to the original BH theory, the ripple pattern formation on irradiated surfaces is a result of an interplay between surface roughening, due to curvature-dependent sputtering yield, and surface smoothing due to thermal diffusion. Although the BH theory was proposed to explain the pattern formation on surfaces of amorphous solids, it was also applied with success to predict morphological structures developing on single-crystal surfaces, which become amorphized during ion irradiation (for example, semiconductor crystals). One of the most valuable achievements of the BH model is the ability to predict the dependence of the ripple alignment on the projectile angle of incidence. However, apart from undisputed achievements, the theory has also several deficiencies. For example, it can explain neither experimentally observed occurrence of a saturation of the surface roughness nor a linear dependence of the ripple wavelength on the projectile's kinetic energy. In contrast to these experimental observations, BH theory predicts an unlimited exponential increase in ripple amplitude and a decrease in their wavelength with the increasing primary ion energy. Recently, Makeev *et al.*[12] generalized Bradley and Harper's second-order linear equation by adding nonlinear and fourth-order terms to address these inadequacies. The generalized theory has introduced an additional ion-induced smoothing mechanism via preferential sputtering without mass movement on the surface.

Most of the studies of ripple formation were done on amorphous surfaces. Much less is known about the dynamics of this process taking place on metal surfaces which preserve their crystallinity during ion irradiation. In order to explain the ripple formation in these systems, Rusponi and co-workers[13,14] modified the nonlinear continuum model for amorphous surface by introducing terms that account for the anisotropic surface diffusion and a presence of step-edge barriers (Ehrlich-Schwoebel barrier). More recently, Hansen *et al.*[15] showed that apart from all these modifications the BH-based continuum theory cannot explain the dynamics of ripple formation on Pt(111) surface under 5 keV Ar^+ bombardment at a grazing incidence. Instead, they have proposed a new model describing evolution of the ripple pattern based on a large difference of the efficiency of sputtering of ascending and descending step edges.

Almost all of the experiments with ripple formation were done on systems in which ejection occurs due to ballistic collisions. There is, however, a wide range of materials such as alkali halides or frozen noble gases, in which erosion can be dominated by electronic processes.[16] Alkali halide crystals are particularly interesting class of materials due to their simple crystallographic and electronic structures. It is also relatively easy to obtain well-characterized single-crystal

surfaces. Finally, the relative contribution of electronic and ballistic processes can be easily tailored in these solids by changing the mass of the projectile,[17] as the relative contribution of electronic processes increases for lighter primary ions. Alkali halides can be used, therefore, as a model system to study development of surface morphology at single-crystal surface under conditions of coexisting electronic and ballistic erosion mechanisms. Within the electronic desorption channel, the excitation energy of the crystal electronic system induced by impinging ions is converted into the kinetic energy of the target constituents by creation of the Frenkel centers.[18] Subsequent diffusion and recombination of these centers at the surface induce ejections of atoms. As the diffusion process is mostly isotropic the morphology development occurs in a manner that reflects predominantly symmetry of the lattice structure, and is insensitive to the direction of the primary ion beam. On the other hand, for oblique incidence, the ballistic processes initiated by a direct momentum transfer retain the memory of the initial impact direction. As a result, under these conditions, ballistic processes can induce anisotropy of the resulting surface morphology.

The aim of the present work is to study the ripple formation on a surface of a single crystal that is simultaneously eroded by both electronic and ballistic processes. A KBr(001) surface was irradiated by low-energy projectiles with two different masses to investigate erosion stimulated mostly by ballistic or electronic processes. We have found that the ion irradiation leads to a formation of well-ordered crystalline ripple structures. For a low-ion fluence, a development of elongated pits together with KBr adislands is observed. This pattern evolves into a well-ordered ripple structure oriented along the ion-beam direction with the increasing time of irradiation. The threshold fluence for the ripple formation depends on the projectile mass. The results are explained by a proposed atomic scale model that combines electronic roughening mechanism with a ballistic roughening attributed to a difference in the erosion rate of the ascending and descending surface step edges.

II. EXPERIMENT

The experiments were performed in UHV system consisting of three interconnected chambers for sample preparation, analysis, and SPM (Scanning Probe Microscopy) imaging. The system enables to perform measurements at very good vacuum conditions. The base pressure in the vacuum chamber was of 5×10^{-11} mbar in all stages of the experiment, including SPM characterization. Maintaining very good vacuum conditions is known to be of crucial importance for studying alkali halide surfaces.[19] Alkali halide crystals purchased from TBL-Kelpin (Neuhausen, Germany) were cleaved in air parallel to the (001) cleavage plane and have been clamped with tungsten springs on a molybdenum plate mounted on a copper sample holder. After mounting, the samples were immediately transferred into the vacuum system for proper cleaning by annealing in UHV at 450 K for several hours. The annealing process is essential in order to remove the adsorbed impurities, and to reduce the stress and charge accumulation.[20] The samples were exposed to focused beams of 4 keV Ar^+ and He^+ ions having the spot size of 1 mm^2. The gas pressure, of high purity argon or helium, in the irradiation chamber during ion gun operation was 1×10^{-6} mbar. The beam has been rastered over the entire surface area. The average ion current density was 1 $\mu A/cm^2$ and the ion fluence, Φ_{ion}, was changed between 10^{13} and 10^{18} ions/cm^2. The incidence angle, α, of the ion beam was $\alpha=75°$ with respect to the surface normal and the azimuthal orientation, i.e., the angle between the projection of the ion beam and the [100] surface direction, was about 45°. The crystal holder was kept at room temperature for all measurements. The resulting surface topographies were analyzed by the atomic force microscopy (AFM) (VP2 Park Scientific Instruments device) in a noncontact mode (nc-AFM) under UHV conditions using the piezoresistive silicon cantilevers of the resonance frequency of 358.4 kHz. The amplitude of oscillation and a nominal tip radius was 10 and 20 nm, respectively. The frequency shift (detuning) relative to the cantilever resonance frequency was set in the range of $-5\div-20$ Hz. For better statistics, the nc-AFM measurements have been done at several different areas of the irradiated sample surface.

Details of molecular-dynamics computer simulations used to model He and Ar bombardment of KBr(001) crystal are described elsewhere.[21] Briefly, the motion of the particles was determined by integrating Hamilton's equations of motion. The forces among the particles were described by a blend of pairwise potential-energy functions. A Born-Mayer-Huggins-Tosi-Fumi potential was used to describe the K^+-Br^-, K^+-K^+, and Br^--Br^- interactions.[22] This potential was splined with a purely repulsive Kr-C potential to better reproduce high-energy collisions.[23] The interactions between the projectile atoms and the rest of the system were described using the purely repulsive Kr-C potential.[23]

The model approximating a flat surface of KBr(001) crystal consists of 68 000 atoms arranged in 21 layers. The direction of the ion beam with its surface component parallel to the [110] crystallographic direction was chosen to reproduce experimental alignment. The lateral dimensions of the sample amount to about 19×19 nm^2. The KBr(001) surface was free and relaxed. The other five sides of the crystal contained three layers of damped atoms in order to simulate thermal environment. The outermost layers were fixed.[21] The sample relaxed to its minimum potential energy was held at 0 K. A surface step oriented along $[1\bar{1}0]$ direction was introduced by removing the left (12.4 nm) or the right part (6.6 nm) of the topmost layer. Projectiles of 4 keV He and 4 keV Ar were directed perpendicular to the step at impact angles of 75° toward the surface normal to reproduce experimental conditions. The processes occurring up to 10 ps after the ion impact were simulated.

III. RESULTS AND DISCUSSION

Figure 1 depicts the development of the surface morphology on KBr(001) single crystal subjected to 4 keV Ar^+ [Fig. 1(a)–1(c)] and 4 keV He^+ [Fig. 1(d)–1(f)] bombardment with the off-normal angle of incidence, $\alpha=75°$ at room tempera-

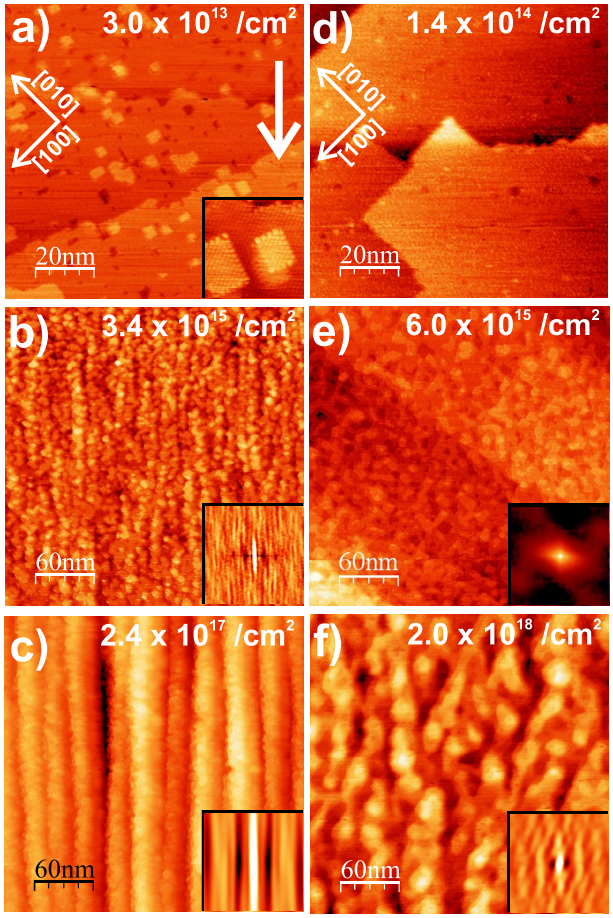

FIG. 1. (Color online) Nc-AFM topographies of KBr(001) surface under 4 keV Ar^+ (a-c) and He^+ (d-f) irradiation as a function of ion fluence [(a)–3.0×10^{13} ions/cm^2, (b) –3.4×10^{15} ions/cm^2, (c) 2.4×10^{17} ions/cm^2, (d) 1.4×10^{14} ions/cm^2, (e) 6.0×10^{15} ions/cm^2, and (f) –2.0×10^{18} ions/cm^2]. The irradiation was performed at room temperature and ion beam has an angle of incidence of $\alpha=75°$ with respect to the surface normal. The white arrow indicates the projection of the ion beam on the irradiated surfaces. The image sizes are 100×100 nm^2 in (a) and (d) and 300×300 nm^2 in (b), (c), (e), and (f). Insets: in (a) atomically resolved image of the KBr adislands (image size 11×11 nm^2), in (b)–(c) and (e)–(f) 2D self-correlation function maps of the topographies shown.

ture (RT). The white arrow in Fig. 1(a) indicates the projection of the ion-beam direction on the irradiated surfaces. This direction was chosen not to coincide with the main [100] and [010] crystallographic surface directions, e.g., there is an azimuthal angle of about 45° between the projection of the ion beam and the [100] direction. Such geometry was chosen in order to distinguish between the influence of the electronic and ballistic processes on the surface morphology development, as it is known that electronic desorption leads to removal of surface atoms along main surface crystallographic directions.[24]

We first consider the case of Ar^+ bombardment. Figure 1(a) presents KBr surface exposed to a low fluence of Ar^+ ions ($\Phi_{ion}=3.0\times10^{13}$ ions/cm^2). As shown in the image, the surface is composed of extended atomic terraces which are separated by monoatomic cleavage steps running across the image. The step contours exhibit a fiordlike shape with elongated clusters of pits oriented in the direction normal to the steps. On the terraces, pits of a monolayer depth coexist with monoatomically high rectangular KBr adislands. Both these features have a rugged shape with local step edges aligned along the main crystallographic directions of the [100] and [010] directions. The atomically resolved nc-AFM imaging reveals that the KBr adislands are of perfect crystallographic order and stechiometry [see inset in Fig. 1(a)]. After additional ion irradiation we observe progressing elongation of individual pits followed by their agglomeration in a form of grooves aligned parallel to the projection of the ion-beam direction [Fig. 1(b), $\Phi_{ion}=3.4\times10^{15}$ ions/cm^2]. As in the case of adislands, the walls of the grooves have a zigzag shape with the local edges bounded to the main, e.g., [100] and [010] crystallographic surface directions. The grooves are separated by the remains of the original topmost layer of the crystal with the adislands located on their top. A closer inspection of Fig. 1(b) shows that at the bottom of the extended pits new vacancy sites are already forming. The extended irradiation leads, finally, to a creation of the ripple structure of the wavelength of 25 nm and the valley-to-peak amplitude of 4 nm, oriented along the ion-beam direction [Fig. 1(c), $\Phi_{ion}=2.4\times10^{17}$ ions/cm^2]. The high-resolution nc-AFM imaging of the ripple ridges shows that they are formed from multilayer atomically high terraces. The terraces are of well-ordered crystalline structure with local edges oriented along the [100] and [010] crystallographic surface directions.

In order to investigate how the relative ratio of the electronic and ballistic processes influence the dynamics of the morphology development, the KBr(001) surface has been irradiated with lighter He^+ ions. The time-of-flight studies of desorption of KI(001) crystal at RT with 5 keV Ar^+ and He^+ ions directed along the surface normal reveal that about 90% and 3% of the desorbed material is emitted by ballistic processes by Ar^+ and He^+ projectiles, respectively.[25] Morphology evolution of KBr(001) surface irradiated with 4 keV He^+ beam at $\alpha=75°$ is shown in Figs. 1(d)–1(f). The evident consequence of a smaller projectile mass is much smaller damage of the irradiated surface. Only for the He^+ ion fluence of 1.4×10^{14} ions/cm^2 [Fig. 1(d)] the appearance of small pits, few nm in lateral size, is observed. Further irradiation leads to expansion of the pits which ultimately results in a removal of the topmost layer. This process is accompanied by simultaneous erosion of the next atomic layer due to creation of vacancies at the bottom of pits, as it was observed during Ar^+ irradiation. Also as in the case of Ar^+ irradiation, the local edges of both the remaining parts of the topmost layer and of the created pits are bound to the main crystallographic directions of the surface. However, in contrary to Ar^+ irradiation, the developed morphology does not exhibit any overall anisotropy [Fig. 1(e), $\Phi_{ion}=6.0\times10^{15}$ ions/cm^2]. Only a very prolonged irradiation leads to creation of shallow groove- and ridgelike structures elongated parallel to the ion-beam direction [Fig. 1(f), $\Phi_{ion}=2.0\times10^{18}$ ions/cm^2]. Formed ripplelike structure, however, is much weaker than observed after Ar^+ bombardment with comparable fluence. It has a wavelength of about 50 nm and the valley-to-peak amplitude of 3 nm.

Within the investigated energy range, the ion sputtering mechanism of alkali halides is usually dominated be electronic processes rather than by ballistic collisions[26,27] due to a very high efficiency of desorption induced by electronic transitions in ionic crystals. This property has a tremendous impact on the evolution of the surface topography exposed to the ion irradiation, as it turns out that there is a close connection between surface topography and desorption yield.[28] In the electron stimulated desorption (ESD) free excitons and electron-hole pairs are created along the ion path due to a high cross section for excitation of the crystal valence band.[29] The excitons and electron-hole pairs self-trapped in the bulk can decay into separate F- and H-center pairs, i.e., an electron trapped into a halogen vacancy (F center) and an interstitial halogen atom (H center). The diffusion of F and H centers and their recombination with the surface lead to the desorption of alkali and halide atoms, respectively.[30] It should be pointed out, however, that surface trapping of only excited-state F centers at low coordination sites (steps and kinks) leads to ejection of surface alkali atoms. The removal of alkali atoms leads, in turn, to a formation of vacancies that may agglomerate into pits.[31] As surface trapping of H centers results in the ejection of excess interstitial halogen atom, this process leaves unmodified surface. Initially, the pits formed by alkali atom removal are two dimensional, growing and overlapping with the increasing ion fluence. Since the surface precursor sites for desorption are localized at the atomic step edges, the pits have natural tendency to expand along the main crystallographic directions of the surface exposing flat areas of the next (deeper) atomic plain. This property explains the observed orientation of the local edges of created structures.

The scenario of ESD desorption presented above leads to the surface erosion in a layer-by-layer mode due to production of vacancies. Therefore, such process is not able to produce adparticles with equal amount of K and Br atoms. We postulate, therefore, that the adislands observed for the oblique Ar^+ irradiation [Fig. 1(a)] are formed due to the ballistic component of sputtering. Indeed, as shown by our computer simulations the impinging ions create numerous KBr admolecules as well as separated K and Br atoms at the surface. These particles can easily diffuse and finally agglomerate into KBr adislands. As the agglomeration takes place on the KBr surface, it is natural to expect for the formed islands to retain KBr surface symmetry. As shown in Fig. 1(a), for 4 keV Ar^+ the adislands cover about 8% of the imaged area, which proves that there is an efficient production of admolecules on the irradiated surface. The contribution of adislands is negligible for 4 keV He^+ ion irradiation. Such behavior is, however, expected for light projectiles as the ballistic energy transfer decreases with an increase in the mass difference between colliding partners.

We recognize twofold effect of the ballistic component of sputtering on erosion of KBr surface. First, impinging projectile can produce separate vacancies on the perfect terraces. This effect can be achieved by either ejection or relocation of the surface atoms from their original positions. Most of these vacancies are one layer deep. However, deeper structures can be also created if the bottom of the pits formed by agglomerated vacancies is hit by another projectile and another atom

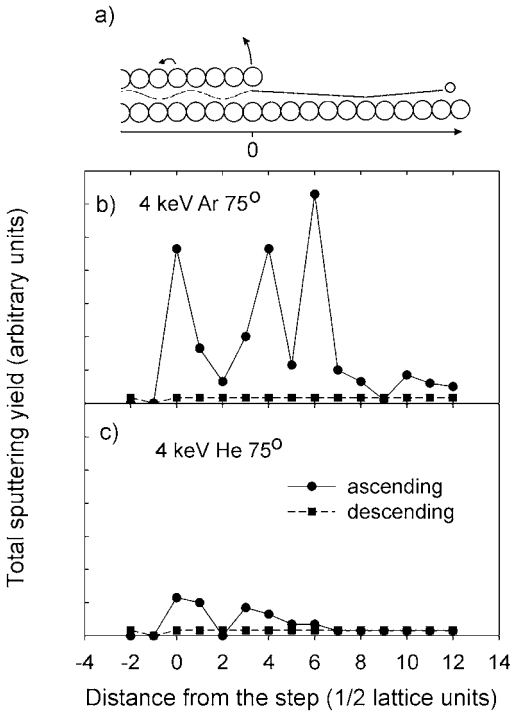

FIG. 2. (a) Schematic sketch of the experimental geometry for the ion irradiation of the terrace/pit step edge. Results of MD simulations of the sputtering yield versus the position of projectile impact at α=75° in vicinity of the ascending (●) and descending (■) step edges for 4 keV Ar are in (b) and for 4 keV He in (c), respectively. The local maxima of the sputtering yield in (b) are due to ions which directly hit the step edge (0 position) or are reflected on the lower terrace and enter the subsurface region between the topmost and underneath atomic layer (positions 4 and 6).

is removed. The created vacancy serves as a trapping site for diffusing excited F centers which leads to ejection of alkali atoms and, consequently, to a development of additional pits. This sputtering channel creates numerous precursor sites for more efficient electronic desorption. This mechanism implies that the surface erosion proceeds in a multilayer mode (simultaneous erosion of few atomic layers) and retains surface lattice symmetry. Since the memory of the initial ion-beam direction is lost during F-center diffusion, this type of surface roughening is insensitive to the direction of the primary ion beam.

However, there is also a second process initiated by a ballistic energy transfer that will lead to a development of surface morphological structures that are dependent on the direction of the ion beam. Namely, as shown in Fig. 2(b), the sputtering efficiency of the ascending and descending step edges illuminated by the oblique ion beam is different. As shown by our molecular-dynamics (MD) simulations, the sputtering yield induced by 4 keV Ar^+ at 75° is almost four times larger from the ascending edge that the same yield calculated in vicinity of the descending edge. A similar result has been observed by Hansen *et al.* for Ar^+ bombardment of single crystal of Pt.[15] This phenomenon is attributed to a planar subsurface sputtering that forces the projectile to move in the subsurface volume. During this movement the projectile stimulates ejection or relocation of numerous sur-

face atoms along its path as shown schematically on Fig. 2(a). Some of these events can occur quite far away from the step edge.[15] This mechanism takes place only for irradiation of the ascending edge. Projectiles irradiating descending edge or side walls of the pits are not channeled. The vacancy sites created during subsurface channeling serve as trapping sites for diffusing excited F centers. This process will additionally enhance total sputtering yield during bombardment of ascending edge, leading to a formation of numerous pits along the path of channeled projectile. These pits will grow fast and merge together due to electronic desorption channel. Both more efficient ejection of atoms from the ascending edge and a formation of expanding pits along trajectory of channeled projectile will lead to a development of surface anisotropy related to the ion-beam direction, which is indeed observed. We would like to emphasize that the development of KBr surface anisotropy will be always related to the ion-beam direction independently of the ion-beam azimuthal direction. As we have already pointed out, the ripple ridges are formed from terraces with local edges aligned along the main [100] and [010] directions. Because the incidence angle is "close" to [110] direction, both local edge directions are equally populated. Then, the change in the azimuthal angle will result in depopulation of one local direction of the ridge in favor of the other main direction. However, the overall direction of the ripples will always follow the ion-beam direction as it is a result of large difference in the erosion rate for the ascending and descending surface step edges.

The relative contribution of isotropic and anisotropic sputtering channels will depend on the mass of the projectile and its angle of incidence. Lighter projectiles are more prone to induce electronic desorption and less prone to stimulate ballistic ejections. As a result, less anisotropic erosion is expected for lighter primary ions. While erosion by electronic roughening should only weakly depend on the incidence angle, the difference between sputtering of ascending and descending edges quickly decreases with a decrease in the impact angle. As a result, one should observe development of more isotropic morphologies at lower impact angles. Our preliminary measurements performed with 4 keV Ar^+ at 30° impact angle indeed confirmed this prediction.

In order to quantitatively characterize the observed ion-induced morphologies, we have calculated so-called *anisotropy factor* of the surface morphology and the root means square roughness (RMS) versus the total ion fluence. The results are shown in Fig. 3. The surface *anisotropy* is defined as the ratio of the parallel and perpendicular, with respect to the ion-beam direction, width of the central peak in a 2D self-correlation function map calculated from the nc-AFM images (the insets in Fig. 1). Thus, the value of the *anisotropy* higher than 1 characterizes surface structures which are elongated along the ion-beam direction, whereas the *anisotropy* lower than 1 corresponds to the elongation in the direction perpendicular to the ion beam. It is clear from Fig. 3(b) that the overall behavior of the surface bombarded by 4 keV Ar^+ and He^+ ion projectiles is somewhat similar, as the development of the surface anisotropy parallel to the primary ion-beam direction is visible in both cases. However, there is also a significant difference. The threshold for the development of anisotropy is shifted to much larger fluence for He^+

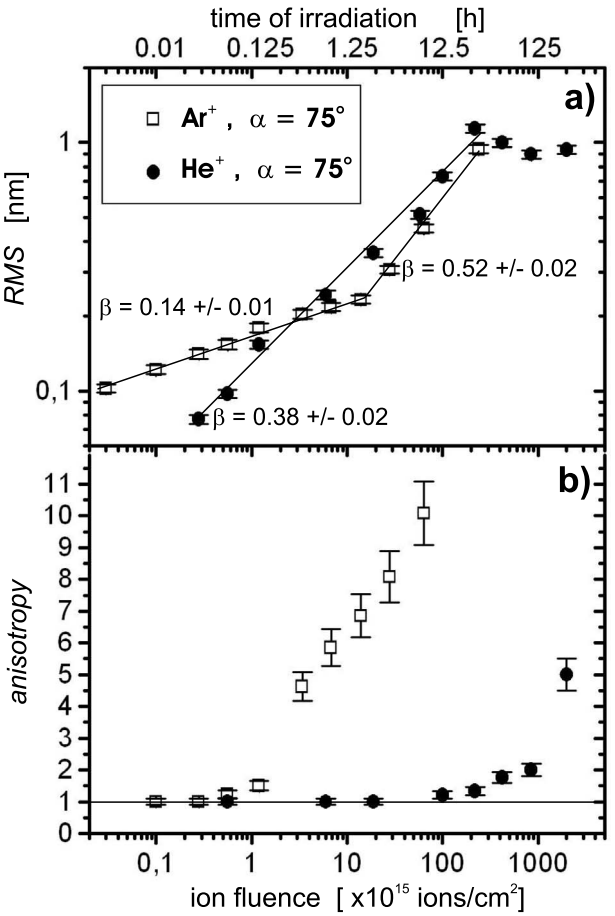

FIG. 3. (a) RMS and (b) *anisotropy* versus the total ion fluence (equivalent to the total time of irradiation) of the ion-induced morphologies of KBr(001) surface under bombardment with 4 keV and $\alpha=75°$ Ar ions (□) and He ions (●) beams. The lines in (a) represent the fits according to the scaling power-law RMS $\sim t^{\beta}$. The corresponding values of growth exponent β are shown in the graph. The *anisotropy factor* is defined as the ratio of the parallel and perpendicular, with respect to the ion-beam direction, width of the central peak in a 2D self-correlation function map.

projectile. This difference can be attributed to a lower contribution of the ballistic sputtering, a lower probability of the surface defect creation by ballistic atom relocation due to a planar channeling in the subsurface volume, and a smaller difference of sputtering yields of ascending and descending edges. While the calculated difference in these sputtering yields is almost 4 for 4 keV Ar^+ at 75° impact angle, barely 1.5 difference is obtained for 4 keV He^+ impact [Fig. 2(c)].

Even larger differences in a behavior of irradiated surface is visible in Fig. 3(a) in which the root mean square (RMS) (Ref. 32) versus the sputtering time (t) is presented. The data indicate that, in general, the RMS scales as RMS $\sim t^{\beta}$ where β is the growth exponent.[33] The KBr surface evolution under the bombardment with He^+ ions can be described with a single $\beta=0.38\pm0.02$ (before saturation of the RMS). Interestingly, for Ar^+ irradiation this dependence cannot be described by a single β. Instead, there is a crossover in the scaling law from $\beta=0.14\pm0.01$ at low-fluence regime (up to 2×10^{16} ions/cm^2) to $\beta=0.52\pm0.02$ at high-fluence irradiation.

How can we understand the observed scaling behavior of the ion-irradiated KBr surfaces? The data presented in Fig. 3(b) show that the irradiation with He^+ ions leads to isotropic surface erosion for a considerably long irradiation time. At this stage of irradiation, the ion-induced morphology develops in a manner reflecting the initial surface symmetry. The anisotropic effects related to the ion-beam direction are small due to a low contribution of the ballistic process to the total sputtering of the crystal. Creation of new vacancy defects at the bottom of the pits form new trapping centers, which can further expand by alkali atom removal due to trapping of diffusing excited F centers, seems to be the main contribution of the ballistic process to the surface erosion. These defects are growing fast as the process is controlled by efficient electronic desorption. This mechanism, in turn, implies that with the increasing time of irradiation there is an increase of the RMS value due to increasing number of simultaneously eroded atomic layers. Finally, at the high-ion fluence, a rough morphology with a considerable concentration of the pit/terrace edges develops allowing for the effect of anisotropic projectile-induced etching of the step edges to be noticeable. As a result, anisotropic structures are created on irradiated KBr surfaces.

The proposed scenario of KBr(001) surface erosion under the He^+ ions impact is supported by the results of Monte-Carlo simulations concerning the erosion of carbon surface with 4 keV Ar^+ ions performed by Koponen *et al.*[34] They have found that RMS of a surface eroded only by atom removal without any relaxation processes scales with the growth exponent of $\beta=0.33\div0.34$. These values are very close to the ones we got for He^+ irradiation where the KBr surface erosion proceeds predominately via electronic processes leading to step atoms removal. The simulations performed by Koponen *et al.* show also that a presence of efficient relaxation processes inducing smoothing of the surface during the ion irradiation affects the growth exponent and shifting it to a lower value $\beta=0.14\div0.17$. As shown in Fig. 3(a) our results for low-fluence irradiation by Ar^+ projectiles can be also described by the same growth exponent. As shown by our MD simulations in this stage of irradiation efficient formation of adatoms and admolecules by ballistic collisions is important. We postulate, therefore, that surface diffusion of these particles is responsible for efficient surface smoothing. The restructuring of the ion beam illuminated steps as well as a filling of ion-induced terrace damages by the diffusing admolecules can be a plausible explanation for the slower roughening of the irradiated surfaces.

For a prolonged irradiation with Ar^+ ions at $\alpha=75°$ we observe the change in a growth characteristic. After a crossover (total fluence about 2×10^{16} ions/cm^2) the growth exponent changes its value to $\beta=0.52\pm0.02$. In Fig. 4, the KBr surface topographies acquired just before and after crossover point are shown. The image collected before the crossover [Fig. 4(a), $\Phi_{ion}=1.4\times10^{16}$ ions/cm^2] shows the relatively smooth KBr surface, as seen in the cross-section profile of the image. At this fluence the pits are already elongated, however, they are still separated. The effect of a preferential erosion of illuminated (ascending) steps resulting in the elongation of the pits in the direction of ion beam dominates the morphology evolution. It seems that the key difference between low- and high-fluence surfaces is the agglomeration of separate pits into three-dimensional vacancy agglomerates, i.e., groovelike structures. We would like to emphasize that desorption mechanism operating in the low-fluence regime by its nature leads to amplification of the surface roughness due to the electronic roughening; the deeper are the grooves, the larger is the number of step-edge precursor sites, the higher is the desorption efficiency leading to new vacancy production. At certain stage of the ion irradiation (the crossover time) separated grooves become to overlap leading to creation of deep groovelike structures of submicrometers length. The appearance of the long grooves is associated with a substantial decrease in the total length of ascending step edges [see Fig. 4(b), $\Phi_{ion}=6.4\times10^{16}$ ions/cm^2] and, consequently, with a decrease in the efficiency of KBr admolecules creation. As a consequence, the smoothing of the surface by diffusing adparticles is reduced and the electronic roughening mechanism starts to dominate the surface evolution and, therefore, the dynamic of the RMS growth is changed.

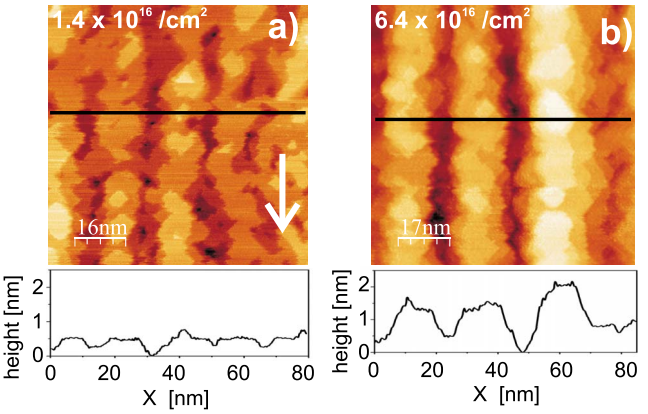

FIG. 4. (Color online) Nc-AFM images of the ion-induced topographies of KBr(001) surface (4 keV Ar^+ ions with $\alpha=75°$) at the two distinguished irradiation time regimes: (a) initial stage of irradiation (total ion fluence 1.4×10^{16} ions/cm^2 and $\beta=0.14\pm0.01$) and (b) the late stage after crossover time (total ion fluence 6.4×10^{16} ions/cm^2 and $\beta=0.52\pm0.02$). The cross-section profiles taken along the lines indicated in the topography images are shown below.

Finally we should mention that there are some similarities between the observed scaling behavior of the ion-irradiated KBr surface and the predictions of a discrete stochastic model of surface erosion by ion sputtering proposed by Cuerno *et al.*[35] In the model, the appearance of the crossover in the scaling behavior of irradiated surfaces associated with change of β for values higher than 0.5 is due to the surface instability caused by a negative surface tension. The negative surface tension implies that the surface tends to maximize its area which, in fact, means that there is an increase in the surface roughness as the ion irradiation proceeds. In standard approaches based on the BH theory, the negative surface tension is associated with the curvature-dependent local erosion yield.[10] Namely, the ions penetrating the solid induce collision cascades along their path. As shown by Sigmund[11] due to a spatial extension of the ion-induced collision cascades the atoms located at the bottom of troughs gain more

energy, on average, than those located on the peaks of crests. As a consequence, the erosion is faster in the depressions than at elevations. In the BH approach, the curvature-dependent sputtering is a mechanism inducing surface instability which finally leads to the ripple formation on the irradiated surfaces.

In some way, we do have analogy between the curvature-dependent sputtering by isotropic collision cascades and the electronic roughening observed in the present case of ion-induced erosion of KBr surface. Similar to the curvature-dependent sputtering, the electronic roughening is a destabilizing mechanism of the irradiated KBr surface. The deeper are the pits the larger is the number of the step-edge precursor sites resulting in the higher desorption efficiency. This, in turn, will lead to creation of new pits. But this is where the analogy ends. Due to the dominance of the electronic erosion channel the KBr surface remains well-ordered even for very large ion fluence. Because of the preserved surface crystallinity, there is a lack of a smooth and continuous variation in the local erosion yield with the surface morphology. These findings together with the lack of the exponential growth of the surface roughness (instead, we observe the scaling behavior of the RMS) imply that none of the basic BH assumptions is fulfilled emphasizing the inapplicability of the continuum theory for the description of the ion-induced ripple formation on KBr surfaces.

IV. CONCLUSIONS

Ion-induced nanostructuring of single crystal KBr(001) surface under bombardment with 4 keV Ar^+ and He^+ beams at 75° angle of incidence has been studied by means of nc-AFM in UHV. It was found that the ion irradiation leads to formation of well-ordered crystalline ripple structures. Ripple structures are oriented along the ion-beam direction. The threshold fluences for the ripple formation depend on the projectile ion mass. It has been found that the electronic roughening is the dominant mechanism which destabilizes the irradiated KBr surface and, finally, leads to periodic structure formation. We have shown that the BH-based continuum theory is inadequate for the description of the mechanism of the ripple formation in the present system. The results are explained by a proposed atomic scale model which combines electronic desorption mechanism with a ballistic roughening attributed to a large difference in the erosion rate of the ascending and descending surface step edges.

ACKNOWLEDGMENTS

The authors would like to thank F. Buatier de Mongeot for fruitful discussions. This work was supported by the Ministry of Science and Higher Education, Poland, Decision No. 268/N-ESF/2008/0 within the Project "Active Control of Friction, ACOF" implemented under the European Science Foundation EUROCORES Programme FANAS (Project Ref. No. 07-FANAS-OP-013_ACOF). Z.P. acknowledges support from the Polish Ministry of Science and Higher Education Program No. PB 4097/H03/2007/33.

*FAX: +48 12 6337086; franciszek.krok@uj.edu.pl

†On leave from Department of Physics, Sulaimani University, City Center 205, Kani-Askan 3, Sulaimani, Kurdistan region, Iraq.

[1] W. L. Chan and E. Chason, J. Appl. Phys. **101**, 121301 (2007).
[2] G. Costantini, F. Buatier de Mongeot, C. Boragno, and U. Valbusa, Phys. Rev. Lett. **86**, 838 (2001).
[3] U. Valbusa, C. Boragno, and F. Buatier de Mongeot, J. Phys.: Condens. Matter **14**, 8153 (2002).
[4] G. Carter and V. Vishnyakov, Phys. Rev. B **54**, 17647 (1996).
[5] A.-D. Brown and J. Erlebacher, Phys. Rev. B **72**, 075350 (2005).
[6] E. Chason, T. M. Mayer, B. K. Kellerman, D. T. McIlroy, and A. J. Howard, Phys. Rev. Lett. **72**, 3040 (1994).
[7] D. Carbone, A. Alija, O. Plantevin, R. Gago, S. Facsko, and T. H. Metzger, Nanotechnology **19**, 035304 (2008).
[8] B. Ziberi, F. Frost, M. Tartz, H. Neumann, and B. Rauschenbach, Appl. Phys. Lett. **92**, 063102 (2008).
[9] T. M. Mayer, E. Chason, and A. J. Howard, J. Appl. Phys. **76**, 1633 (1994).
[10] R. M. Bradley and J. M. Harper, J. Vac. Sci. Technol. A **6**, 2390 (1988).
[11] P. Sigmund, J. Mater. Sci. **8**, 1545 (1973).
[12] M. A. Makeev, R. Cuerno, and A.-L. Barabasi, Nucl. Instrum. Methods Phys. Res. B **197**, 185 (2002).
[13] S. Rusponi, G. Costantini, C. Boragno, and U. Valbusa, Phys. Rev. Lett. **81**, 4184 (1998).
[14] S. Rusponi, G. Costantini, C. Boragno, and U. Valbusa, Phys. Rev. Lett. **81**, 2735 (1998).
[15] H. Hansen, A. Redinger, S. Messlinger, G. Stoian, Y. Rosandi, H. M. Urbassek, U. Linke, and T. Michely, Phys. Rev. B **73**, 235414 (2006).
[16] Z. Postawa, R. Maboudian, M. El-Maazawi, M. H. Erwin, M. C. Wood, and N. Winograd, J. Chem. Phys. **96**, 3298 (1992).
[17] Z. Postawa, Radiat. Eff. Defects Solids **128**, 107 (1994).
[18] M. Szymonski, Nucl. Instrum. Methods Phys. Res. B **46**, 427 (1990).
[19] R. M. Wilson and R. T. Williams, Nucl. Instrum. Methods Phys. Res. B **101**, 122 (1995).
[20] C. Barth and C. R. Henry, Nanotechnology **15**, 1264 (2004).
[21] B. J. Garrison and Z. Postawa, Mass Spectrom. Rev. **27**, 289 (2008).
[22] M. Tosi and F. Fumi, J. Phys. Chem. Solids **25**, 45 (1964).
[23] W. D. Wilson and L. G. Haggmark, Phys. Rev. B **15**, 2458 (1977).
[24] R. Bennewitz, S. Schar, V. Barwich, O. Pfeiffer, E. Meyer, F. Krok, B. Such, J. Kolodziej, and M. Szymonski, Surf. Sci. **474**, L197 (2001).
[25] S. W. Rosencrance, D. E. Riederer, R. Chatterjee, C. He, N. Winograd, and Z. Postawa, Nucl. Instrum. Methods Phys. Res. B **101**, 137 (1995).
[26] F. Krok, J. J. Kolodziej, B. Such, P. Czuba, P. Piatkowski, P. Struski, and M. Szymonski, Nucl. Instrum. Methods Phys. Res.

B **226**, 601 (2004).
[27] S. R. Saeed, O. P. Sinha, F. Krok, and M. Szymonski, Appl. Surf. Sci. **255**, 1766 (2008).
[28] B. Such, J. Kolodziej, P. Czuba, P. Piatkowski, P. Struski, F. Krok, and M. Szymoński, Phys. Rev. Lett. **85**, 2621 (2000).
[29] M. Szymonski, K. Dan. Vidensk. Selsk. Mat. Fys. Medd. **43**, 495 (1993).
[30] M. Szymonski, J. Kolodziej, B. Such, P. Piatkowski, P. Struski, P. Czuba, and F. Krok, Prog. Surf. Sci. **67**, 123 (2001).
[31] V. Puchin, A. Shluger, Y. Nakai, and N. Itoh, Phys. Rev. B **49**, 11364 (1994).
[32] We assume that due to the atomically sharp tip apex (atomically resolved nc-AFM images, at least in the *Z* direction) the RMS values exhibit the inherent properties of the developed morphologies not influenced by the convolution with the tip shape.
[33] A.-L. Barabasi and H. E. Stanley, *Fractal Concepts in Surface Growth* (Cambridge University Press, Cambridge, 1995).
[34] I. Koponen, M. Hautala, and O.-P. Sievanen, Phys. Rev. B **54**, 13502 (1996).
[35] R. Cuerno, H. A. Makse, S. Tomassone, S. T. Harrington, and H. E. Stanley, Phys. Rev. Lett. **75**, 4464 (1995).